Available online at www.sciencedirect.com
ScienceDirect
Electrochimica Acta 52 (2007) 7183–7192
ELECTROCHIMICA Acta
www.elsevier.com/locate/electacta

Surface analysis of inhibitor films formed by 1-aminoanthraquinones on API 5L-X60 steel in diesel–water mixtures

N. Muthukumar [a,*], A. Ilangovan [b], S. Maruthamuthu [a], N. Palaniswamy [a]

[a] *Central Electrochemical Research Institute, Karaikudi 630006, India*
[b] *School of Chemistry, Bharathidasan University, Trichirappalli 620024, India*

Received 10 January 2007; received in revised form 5 May 2007; accepted 11 May 2007
Available online 21 May 2007

Abstract

Three long chain fatty acid substituted aminoanthraquinone (AAQ) were synthesized in the laboratory and evaluated as corrosion inhibitors for steel (API 5L-X60) in diesel–water mixtures at room temperature by weight loss and electrochemical studies. Potentiodynamic polarization studies carried out at room temperature on steel (API 5L-X60) in diesel with water containing 120 ppm of chloride and 50 ppm of aminoanthraquinone (AAQ) derivative showed that all the investigated compounds are of anodic type. The results obtained indicate that 1-aminoanthraquinone derivatives are good corrosion inhibitors in diesel–water mixtures. Oleic acid substituted aminoanthraquinone was found to be the best corrosion inhibitor. It exhibited 92% inhibition efficiency against the corrosion of API 5L-X60 steel in diesel–water mixtures. The surface analysis by AFM indicates the adsorption of synthesized inhibitors on the metal surface.

Keywords: Fatty acid substituted aminoanthraquinone; Corrosion inhibition; Diesel–water; Steel API 5L-X60

1. Introduction

The petroleum industry suffers from the economic losses derived from the serious damages caused by metallic corrosion of piping and plant systems. Statistical data show that failures by corrosion in the oil and gas industry oscillate between 25 and 30% of the total losses [1–3]. There are many methods available to prevent the corrosion of piping and plants in aggressive environments where one of the most economic methods is the application of corrosion inhibitors (CIs) [4–7]. Organic compounds are used as typical oilfield corrosion inhibitors function by forming a film or protective barrier between metal and the corrosive fluid either because of their anodic, cathodic or mixed type behaviour [8,9]. Alkenyl phenones [10], aromatic aldehydes [11], nitrogen containing heterocyclic and their quaternary salts [12], and condensation products of carbonyls and amines [13] are commonly used as oil field corrosion inhibitors. In oil transporting pipelines, stagnation of water occurs due to the slopes in the landscape and this acts as a breeding ground for bacteria. Now it is well established that bacterial species exist in oil pipeline and degrade petroleum to maintain their life cycle [14,15] and leads to severe corrosion problems [16]. Mitigation of oil pipeline corrosion still remains as a daunting challenge and continuous efforts are being made to solve or minimize this problem.

Quinones take part in several biological processes such as photosynthesis and respiration. In certain biomembrane assemblies, they are part of electron transfer chains, for example in mitochondrial respiration, this role is played by ubiquinone or coenzyme Q [17]. Anthraquinone derivatives have been employed as dyes [18], chemical sensors [19], organogelators [20], mesogens [21–26], anticancer agents [27], but not yet as a corrosion inhibitor. Thus it is envisaged that it is possible to influence this phenomenon by, such as quinone derivatives [28]. In continuation on the development of corrosion inhibitors, three long chain fatty acids substituted (octanoic acid, decanoic acid,

* Corresponding author. Tel.: +91 4565 227550; fax: +91 4565 227779.
E-mail address: muthu12kumar@yahoo.co.in (N. Muthukumar).

0013-4686/$ – see front matter © 2007 Elsevier Ltd. All rights reserved.
doi:10.1016/j.electacta.2007.05.036

oleic acid) aminoanthraquinone have been synthesized (compounds **5**–**7**) with an objective to study their corrosion inhibiting properties on API 5L-X60 steel in diesel–water mixtures. The selection of these compounds as corrosion inhibitors is based on the facts that these compounds contain lone pair of electrons on N atoms and π electrons in aromatic ring through which they can adsorb themselves on the metal surface. The lateral interaction of long chain of carbon atoms due to Van der Waal forces can further facilitate formation of compact film of inhibitor on the metal surface [29]. In the present study, the mechanism of 1-aminoanthraquinone derivatives on corrosion inhibition has been investigated.

2. Experimental procedure

2.1. Materials

Octanoic acid, decanoic acid, oleic acid, 1-aminoanthraquinone, potassium carbonate, thionyl chloride and dimethylformamide and acetone obtained from Aldrich, were used for the synthesis of 1-aminoanthraquinone derivatives. All the used solvents were of HPLC grade.

2.2. Preparation of inhibitors

Methods reported for the synthesis of 1-aminoanthraquinone derivatives or its closely related variants. 1-Stearoyl, 1-palmitoyl, and 1-lauroyl aminoanthraquinone derivatives were prepared in very poor yield ranging from 2 to 6.5% by treatment of 1-aminoanthraquinone with different acid chlorides in the presence of solvent nitrobenzene [30]. Similarly 1,4-diamidoanthraquinone derivative were obtained by treatment of acyl chlorides with amine in the presence of pyridine in *N*,*N*-dimethylacetamide solvent in moderate to good yield [31]. In the present study, synthesis of different quinone derivatives **5**–**7**, with long alkyl chain was planned. Quinone derivatives **5**–**7** were prepared by treatment of compound **1** with acid chlorides **2**–**4** in the presence of potassium carbonate (K_2CO_3) containing acetone and refluxed to give the corresponding amides in high yield (Scheme 1). Different acid chlorides needed for the synthesis were prepared from corresponding acid using equivalent quantity of thionyl chloride ($SOCl_2$) in presence of few drops of *N*,*N*-dimethylformamide (DMF) in benzene as solvent. All the products were obtained as yellow solid with characteristic melting point.

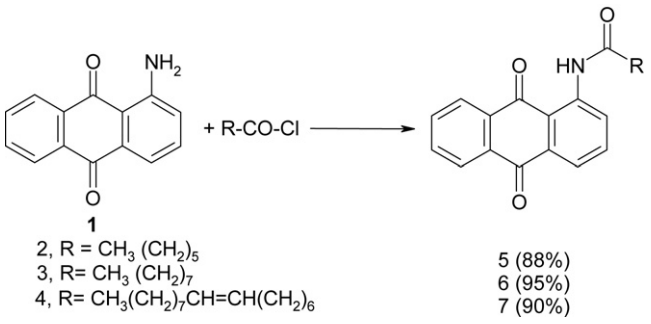

Scheme 1.

2.2.1. Preparation of octanoic acid (9,10-dioxo-9,10-dihydro-anthracen-1-yl)-amide (compound **5**)

2.2.1.1. Part 1. Preparation of octanoyl chloride. Octanoic acid (3.25 g, 0.0225 mol) was allowed to react with thionyl chloride (2.67 g, 0.0225 mol) in benzene (10 mL) and four drops of DMF. The reaction was endothermic and stirred for 10 min and then heated in an oil bath for 1 h at 60 °C, and taken as such for further reaction followed in part 2.

*2.2.1.2. Part 2. Preparation of octanoic acid (9,10-dioxo-9,10-dihydro-anthracen-1-yl)-amide (**5**).* A mixture of 1-aminoanthraquinone **1** (3 g, 0.0134 mol) and potassium carbonate (3.68 g, 0.0268 mol) was taken in acetone (30 mL) and stirred at room temperature for 45 min. Octanoyl chloride, prepared as described in part 1, was added in 15 min to the reaction mixture. The reaction mixture was stirred at reflux temperature for 3 h (TLC, hexane: ethyl acetate, 7:3, $R_f = 0.4$) and then allowed to attain the room temperature. The reaction mixture was poured into water (100 mL) and ethylacetate (20 mL) was added and then taken in to a separating funnel. The organic layer was separated out and the aqueous layer was washed with ethylacetate (2 × 20 mL). The combined organic layer was washed with $NaHCO_3$ (2 × 20 mL) and dil. HCl (2 × 20 mL), water (20 mL) then dried with Na_2SO_4. Organic layer was concentrated to afford octanoic acid (9,10-dioxo-9,10-dihydro-anthracen-1-yl)-amide in 95% yield as a yellow solid. mp 132–134 °C.

IR (*KBr*): –N–H str (3235.29 cm^{-1}), –C–H str (2926.26 cm^{-1}), amide >C=O (1702 cm^{-1}), quinone >C=O (1643.53, 1667.57 cm^{-1}), aromatic–C–H (1579.57, 1528.88 cm^{-1}), –C–N bond (1266.88 cm^{-1}). *UV* (*$CHCl_3$*): 330 (2.50), 414 (4.49).

^{1}*H NMR* (400 MHz, $CDCl_3$): δ 12.351 (s, 1H), 9.119–9.151 (m), 8.924–8.261 (m), 8.081–8.036 (m), 7.859–7.729 (m, 7H attached to C_2, C_3, C_4, C_5, C_6, C_7, C_8), 2.592 (t, 2H), 1.859–1.788 (m, 2H), 1.385–1.320 (m, 8H), 0.919–0.858 (t, 3H).

The same methodology was followed for the preparation of compounds **6** and **7** (decanoic acid and oleic acid substituted aminoanthraquinone derivatives).

2.3. Spectral characterization of inhibitors

All the products obtained were completely characterized using nuclear magnetic resonance spectroscopy (NMR), Fourier transform infrared spectroscopy (FTIR) and ultra visible spectrophotometer (UV) studies. The FTIR spectroscopy was used to detect the functional group of compounds. PAR Elmer, UK make, Paragon 500 model FTIR was used for the analysis of the corrosion inhibitors. The spectrum was taken in the mid IR region of 400–4000 cm^{-1} with 16-scan speed. The samples were mixed with spectroscopically pure KBr in the ratio of 1:100 and pellets were fixed in the sample holder and the analyses were carried out. ^{1}H NMR spectra were measured in a solvent of deutrated choloroform ($CDCl_3$), containing 0.1% (v/v) of tetramethylsilane (TMS) as an internal standard. The chemical shifts (δ) were reported in ppm and the coupling constants (*J*) in Hz. All experiments were performed on a Bruker 400 MHz

spectrometer. UV–vis spectra were carried out on CARY 500 scan UV–vis spectrophotometer with $CHCl_3$ as solvent.

2.4. Cyclic voltammetry study

The electron transfer mediator properties of quinone derivatives of **5–7** were studied by cyclic voltammetry. Cyclic voltammetry was recorded in 0.1 M, $(CH_3CH_2CH_2CH_2)_4NClO_4$ (tetrabutylammonium perchlorate) containing 0.005 M aminoanthraquinone derivatives in DMF (*N*,*N*-dimethylformamide), scanned within potential window of 0 to −2 V, at the sweep rate of 50 mV/s after purging the solution with N_2 gas to remove dissolved oxygen. Glassy carbon, Pt foil, Ag/AgCl was used as working, auxiliary and reference electrodes, respectively. Cyclic voltammetry was carried out using 'Pine' instrument and $K_3[Fe(CN)_6]$ in 0.1 M KCl standard was used to check the instrument.

2.5. Corrosion studies

2.5.1. Weight loss study

After the preparation, corrosion inhibition efficiency for aminoanthraquinone derivatives **5–7** was evaluated using weight loss method. The chemical composition of the steel API 5L-X60 grade steel specimen is shown in Table 1. Steel coupons of size 2.5 cm (l) × 2.5 cm (b) × 0.5 cm (t) were mechanically polished to homogeneous surface and then degreased using trichloroethylene (ASTM G1-90) [32]. Control system consisting of 500 mL of diesel with 2% of water containing 120 ppm of chloride ion was made to mimic the oilfield pipeline environment. Quinone derivatives **5–7** (different concentrations) were added in experimental system. Three mild steel specimens were immersed into each system and the synthesized inhibitors were evaluated by ASTM standard (G 170) reported by Papavinasam et al. [33] for a period of 10 days. After inoculation period, the coupons were removed and pickled, washed with water and dried by air drier. Final average weight loss values for three coupons were taken and the corrosion rate was calculated.

2.5.2. Electrochemical studies

The electrochemical experiments were made using a conventional three-electrode cell assembly at 28 ± 1 °C. All the solutions were prepared using AR grade chemicals using triple distilled water and was deaerated by purging purified nitrogen for half an hour before the start of the experiments. The working electrode was a steel (API 5L-X60) sample of 1 cm^2 area and the rest being covered with araldite epoxy. A large rectangular platinum foil was used as counter electrode and saturated calomel electrode as the reference electrode. The working electrode was polished with different grades of emery papers, washed with water and degreased with trichloroethylene. The polarization and impedance studies were made after 30 min of immersion using Solatron Electrochemical Analyzer (Model 1280 B). The polarization was carried out using a Corware software from a cathodic potential of −0.2 V to an anodic potential of +0.2 V with respect to the corrosion potential at a sweep rate of 0.5 mV/s. The data in the Tafel region (−0.2 to +0.2 V versus corrosion potential) have been processed for evaluation of corrosion kinetic parameters. The linear Tafel segments of the anodic and cathodic curves were extrapolated to corrosion potential for obtaining the corrosion current values.

Table 1
Chemical composition (wt.%) of API 5L-X60 steel

Sl. no.	Element	Weight (%)
1	C	0.26
2	S	0.05
3	P	0.04
4	Mn	1.35
5	Fe	Balance

The inhibition efficiency was evaluated from the measured i_{corr} values using the following relationship:

$$\mathrm{IE}\,(\%) = \left\{ \frac{i_{corr} - i'_{corr}}{i_{corr}} \right\} \times 100 \quad (1)$$

where i_{corr} and i'_{corr} are the corrosion current values without and with the addition of various concentrations of aminoanthraquinone derivatives.

The impedance measurements were carried out using ac signals of 10 mV amplitude for the frequency spectrum from 100 kHz to 0.01 Hz. Marquardt's model [34] based on Taylor series expansion, a nonlinear fitting technique was applied for calculating impedance parameters. A mixture of petroleum and water (containing 120 ppm chloride ion) in the ratio of 2:1 was made [35]. In each system two mild steel specimens were immersed and stirred vigorously for a period of 7 days. After the test period, electrochemical tests were carried out in a special cell containing aqueous medium collected from experimental system. Impedance and polarization were carried out by employing water used after 7 days period of stirring system.

2.6. Atomic force microscope (AFM)

The API 5L-X60 specimens of size 1.0 cm × 1.0 cm × 0.06 cm were abraded with emery paper (grade 320-500-800) to give a homogeneous surface, then washed with distilled water and acetone. After immersion in diesel–water mixture in the presence and in the absence of 50 mg L^{-1} aminoanthraquinone derivative at 30 °C for 8 h, the specimen was dried in room temperature, and then characterized by atomic force microscopy. Pico scan 2100 model (Molecular Imaging, USA) using gold coated SiN_3 cantilevers (force constant 3 n/W) of 30 nm tip area. AFM pictures were realized in contact mode.

3. Results and discussions

3.1. Characterization of synthesized inhibitors

Addition of long alkyl chain gave raise to good solubility of 1-aminoanthraquinone derivatives **5–7** in petroleum products as well as non-polar organic solvents, such as benzene, toluene and

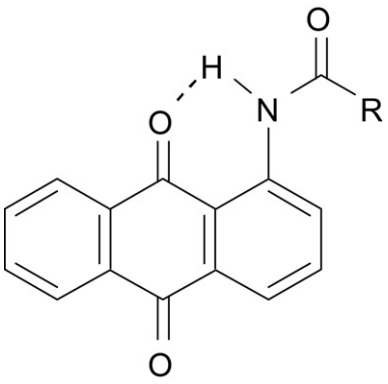

Scheme 2.

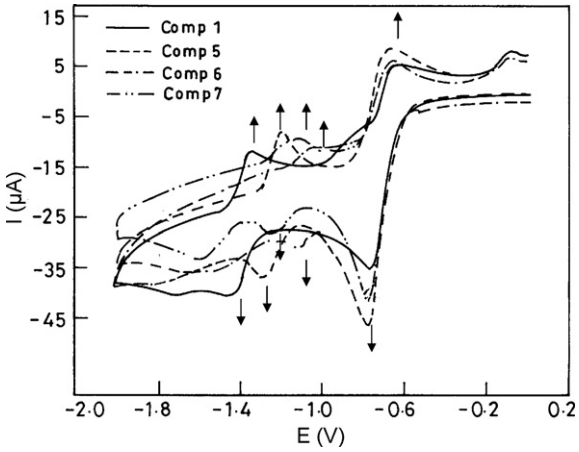

Fig. 1. Cyclic voltammograms of AAQ derivatives (0.005 M) on a glassy carbon electrode in a nonaqueous *N*,*N*-dimethylformamide (DMF) at a scan rate 50 mV/s [arrow indicates the redox potential of the synthesized AAQ derivatives (**5**–**7**)].

tetrahydrofuran (THF). The solubility increases proportionately with increase in alkyl chain length. All the quinone derivatives obtained were characterized using NMR, FTIR and UV studies.

^{1}H NMR, for quinone derivatives **5**–**7**, recorded in $CDCl_3$, showed a triplet for terminal methyl $–CH_3$ group around 0.919–0.858 ppm, multiplet for CH_2 groups around 1.32–1.38 and 1.78–1.85 ppm, $–CH_2$ group adjacent to –C=O as a triplet around 2.59 ppm, seven protons for anthraquinone aromatic ring around 9.13–9.15 ppm, 8.92–8.26 ppm (m), 8.08–8.03 ppm (m), 7.85–7.72 ppm (m), and for compounds **5**–**7** –N–H amide proton were observed as a singlet around 12.35 ppm. It confirms the introduction of acyl groups to the basic 1-aminoanthraquinone core. IR spectra for compounds **5**–**7**, showed –N–H signals in the range at 3208–3350 cm^{-1}. It indicates that the starting material 1-aminoanthraquinone has a primary amine group, which has been transferred into amide form in the synthesized compounds (**5**–**7**). Three carbonyl frequencies corresponding to amide –C=O, hydrogen bonded C=O and non-hydrogen bonded C=O could be observed in the region 1701–1703, 1665–1668 and 1643–1645 cm^{-1}, respectively. It is due to the influence of strong electron withdrawing nature of quinone function.

Scheme 2 indicates the intramolecular hydrogen bonding in 1-aminoanthraquinone derivatives [36]. The introduction of strong electron withdrawing amide group has lead to the hypsochromic yellow shift in absorption frequencies as noticed from its UV spectral data. This could be also due to amide –C=O trying to compete with quinonic –C=O group and weaken the intramolecular hydrogen bonding. It supports the observations made by Philipovaa et al. [37].

3.2. Cyclic voltammetry

Electron transfer mediator properties of quinone derivatives of **5**–**7** were studied by cyclic voltammetry (Fig. 1). The reduction sweep (cathodic) for all the derivatives consist of two major reversible (or quasi-reversible) reduction waves (Table 2). The electrochemical transitions consist of two consecutive one-electron reduction steps [38] of anthraquinone (AQ) to generate first the semiquinone radical anion $AQ^{\bullet -}$ and then the dianion AQ^{2-}, while the third reduction step is attributed to a rapid complex formation between species involved in the course of CV reduction [39]. The quinone derivatives **5**–**7** displayed less negative reduction potentials compared to 1-amionoanthraquinone, thus will be able to accept electrons easily. It is known that electron-withdrawing substituents such as amido groups will tend to shift the reduction potential of the anthraquinone to less negative potentials [39]. However, the presence of hydrogen bonding between quinonic –C=O and amide –NH bond will tend to make the other carbonyl group difficult to undergo reduction. Thus the second reduction potential is observed at higher value than the first one. This is another indication for the existence of intramolecular hydrogen bonding in quinone derivatives **5**–**7**.

3.3. Corrosion studies

3.3.1. Weight loss study

The inhibition efficiency of aminoanthraquinone derivatives is presented in Table 3. The highest corrosion inhibition (92%) was noticed in presence of compound **7** (C_{18} side chain) when compared to other synthesized compounds **5** and **6**. This is for the first time a quinone derivative was found to show corrosion inhibition properties in diesel–water mixtures. Besides, as the chain length increases the corrosion inhibition efficiency increased proportionately.

3.3.2. Electrochemical studies

The potentiodynamic polarization behaviour in the Tafel region for steel (API 5L-X60) in diesel–water mixture

Table 2
Redox potential of AAQ derivatives (compounds **5**–**7**) measured by cyclic voltammetry

Sl. no.	Compound	V vs. Ag/AgCl			
		E_2^c	E_2^a	E_1^c	E_1^a
1	**1**	−1.440	−1.340	−0.780	−0.650
2	**5**	−1.355	−1.195	−0.765	−0.640
3	**6**	−1.205	−1.130	−0.760	−0.650
4	**7**	−1.260	−1.200	−0.720	−0.660

Table 3
Corrosion inhibition efficiency of AAQ derivatives (compounds **5**–**7**) evaluated by weight loss method

Concentration of inhibitor (ppm)	Octanoic acid substituted (C_8) AAQ {compound **5**}			Decanoic acid substituted (C_{10}) AAQ {compound **6**}			Oleic acid substituted (C_{18}) AAQ {compound **7**}		
	Weight loss (mg)	Corrosion rate (mm/year)	IE (%)	Weight loss (mg)	Corrosion rate (mm/year)	IE (%)	Weight loss (mg)	Corrosion rate (mm/year)	IE (%)
Blank	72.5	0.2603	–	72.5	0.2603	–	72.5	0.2603	–
25	42.3	0.1519	42	40.1	0.1440	45	28.9	0.1038	60
50	35.6	0.1278	51	33.5	0.1202	54	7.7	0.0276	89
100	29.4	0.1056	59	27.2	0.0977	63	5.8	0.0208	92

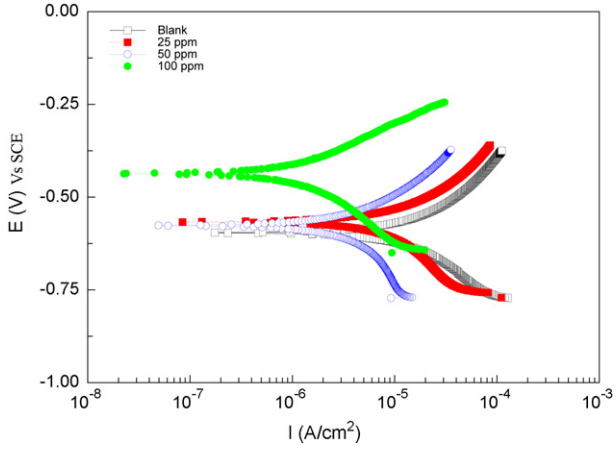

Fig. 2. Polarization behaviour of API 5L-X60 steel in diesel–water mixtures in presence and absence of AAQ derivative (compound **5**).

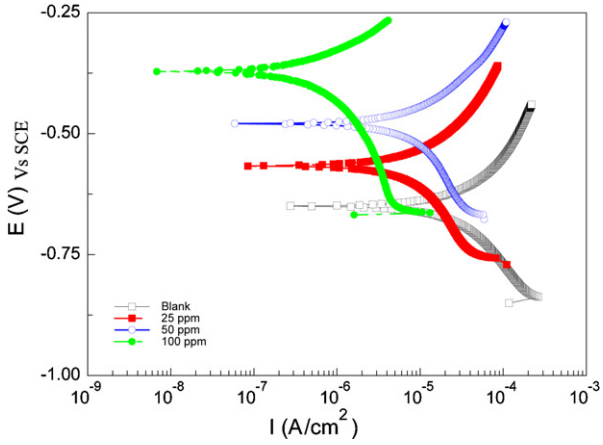

Fig. 3. Polarisation behaviour of API 5L-X60 steel in diesel–water mixtures in presence and absence of AAQ derivative (compound **6**).

in the ratio of 2:1, with and without the addition of various concentrations of 1-aminoanthraquinone derivatives is shown in Figs. 2–4. The corrosion kinetic parameters such as corrosion potential (E_{corr}), corrosion current density (i_{corr}) and Tafel constants (b_a and b_c) derived from these figures are presented in Table 4. The inhibition efficiencies increased with increasing the concentration of the 1-aminoanthraquinone derivatives. The corrosion current density (i_{corr}) values decreased from 13.85 μA/cm^2 of the blank to 9.62, 3.93 and, 1.16 μA/cm^2, in the addition of 25, 50, 100 ppm concentrations of octanoic acid (C_8) substituted 1-aminoanthraquinone (AAQ) derivative (compound **5**), respectively. The corrosion current density (i_{corr}) values decreased from 13.85 μA/cm^2 of the blank to, 1.09, 0.66 and 0.37 μA/cm^2, in the addition of 25, 50, 100 ppm concentrations of decanoic acid (C_{10}) substituted AAQ derivative (compound **6**), respectively, while adding oleic acid (C_{18}) substituted aminoanthraquinone derivative (compound **7**), the corrosion current density (i_{corr}) values decreased to 9.25, 3.16 and 0.05 μA/cm^2, in the addition of 25, 50, 100 ppm concentrations, respectively.

Table 4
Electrochemical parameters for the corrosion of steel API 5L-X60 in diesel–water mixtures in presence and absence of AAQ derivatives (compounds **5**–**7**)

Concentration of AAQ derivatives (ppm)	E_{corr} (mV vs. SCE)	b_a (mV/dec)	b_c (mV/dec)	I_{corr} (μA/cm^2)	IE (%)
Blank	−596	187	194	13.85	
Compound **5**					
25	−566	170	192	9.62	31
50	−576	163	182	3.93	72
100	−436	129	191	1.16	92
Compound **6**					
25	−650	195.2	195.4	9.25	33
50	−479	108.1	208.2	3.16	77
100	−372	151.7	272.8	0.05	99
Compound **7**					
25	−488	135	225	1.09	92
50	−405	154	210	0.66	95
100	−394	72	198	0.37	97

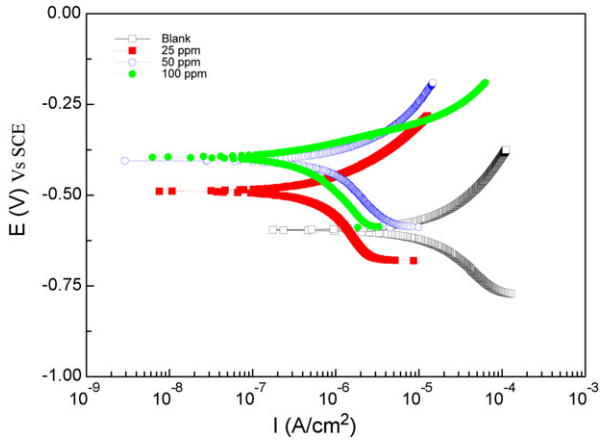

Fig. 4. Polarisation behaviour of API 5L-X60 steel in diesel–water mixtures in presence and absence effect of AAQ derivative (compound **7**).

The Nyquist plots of the impedance values of the steel (API 5L-X60) in diesel–water mixtures with and without the addition of various concentrations of AAQ derivatives are presented in Figs. 5–7 and in Table 5. Single capacitive loop was noticed in the absence of inhibitor system (blank). Two capacitive loops were noticed while adding the inhibitor. The first loop was characterized by a relatively small-flattened loop added to second. The first capacitive loop was well defined in the high frequency (HF) range. The low frequency (LF) part of the diagram was not clearly defined. The HF part curve indicates the intact part of the adsorbed film, whereas the LF data points are associated with the Faradaic process occurring on the bare metal through defects and pores [40–42] in the adsorbed inhibitor layer. Nyquist plots of API 5L-X60 in diesel–water mixtures consist of two semicircles in different ranges and can be analysed by an equivalent circuit, which is represented in Fig. 8.

The respective Bode modulus plots are shown in Figs. 5b, 6b and 7b. The electrode impedance greatly increased from 25 to 100 ppm when compared to control (blank) experiment. The Bode phase angle θ versus log frequency plots show (Figs. 5–7) the phase shift in the high frequency side for 100 ppm of AAQ derivatives (compounds **5**–**7**), which is an indication of the inhibitive nature of the synthesized compounds [43,44]. This is in agreement with the results of polarization data. The capacitance values were lower in all inhibitor addition systems when compares to control. It also confirms that the adsorbed film reduces the dielectric constant present on the metal surfaces. The decrease in C_{dl} values in the presence of inhibitors such as propyl amine (PA), isopropyl amine (*i*-pA), etc., for steel in petroleum–water mixture medium has been reported by many investigators [45–47]. Decrease in the C_{dl}, which can result from a decrease in local dielectric constant and/or an increase in the thickness of the electrical double layer suggests that the inhibitors adsorb at the metal–solution interface [48,49].

3.4. AFM measurement

The atomic force microscope is a powerful means of characterizing the surface morphology [50–53]. The adsorption

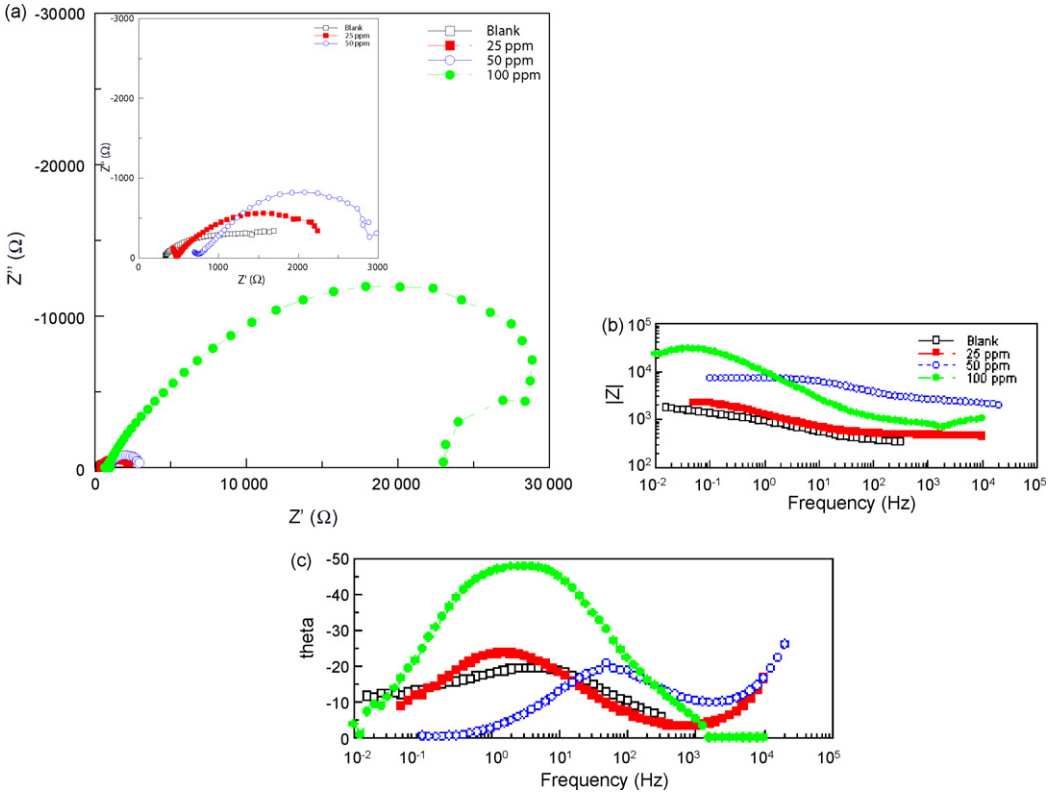

Fig. 5. Impedance diagram (a) Nyquist plots, (b) Bode modulus and (c) Bode phase angle plots diagrams for API 5L-X60 steel in diesel–water mixtures containing different concentrations AAQ derivative (compound **5**).

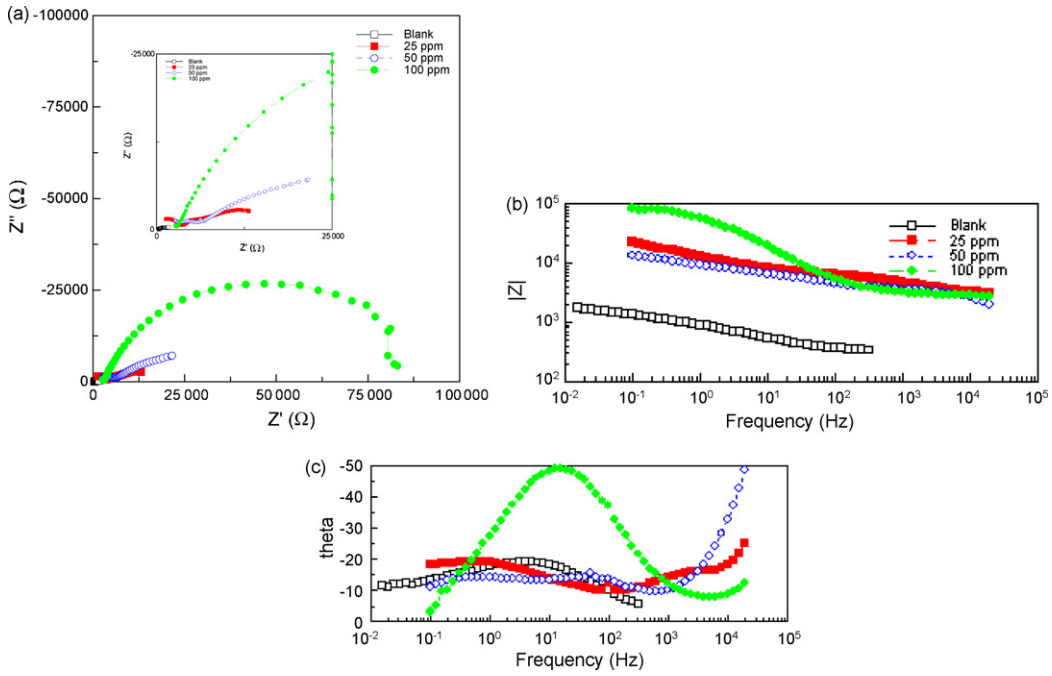

Fig. 6. Impedance diagram (a) Nyquist plots, (b) Bode modulus and (c) Bode phase angle plots diagrams for API 5L-X60 steel in diesel–water mixtures containing different concentrations AAQ derivative (compound **6**).

process due to the action of 1-aminoanthraquinone derivative (compound **7**) was monitored with an AFM in 8 h immersion time and presented in Figs. 9 and 10. The surface morphology of the sample before exposure to aminoanthraquinone derivatives is presented in Fig. 9. Fig. 10 shows a thin and covering surface film composed of many particles. Fig. 10a shows the spherical or bread-like particles appear on the surface, which does not exist in the Fig. 9a. Investigation by Leng and Stratmann [54] suggested that adsorption of corrosion inhibitors may form a few protective monolayers. These particles may be mainly composed of the adsorbed aminoanthraquinone derivative molecule.

3.5. Mechanism proposed

Generally all petroleum product pipelines have water contamination in the range between 2–11%. It can be con-

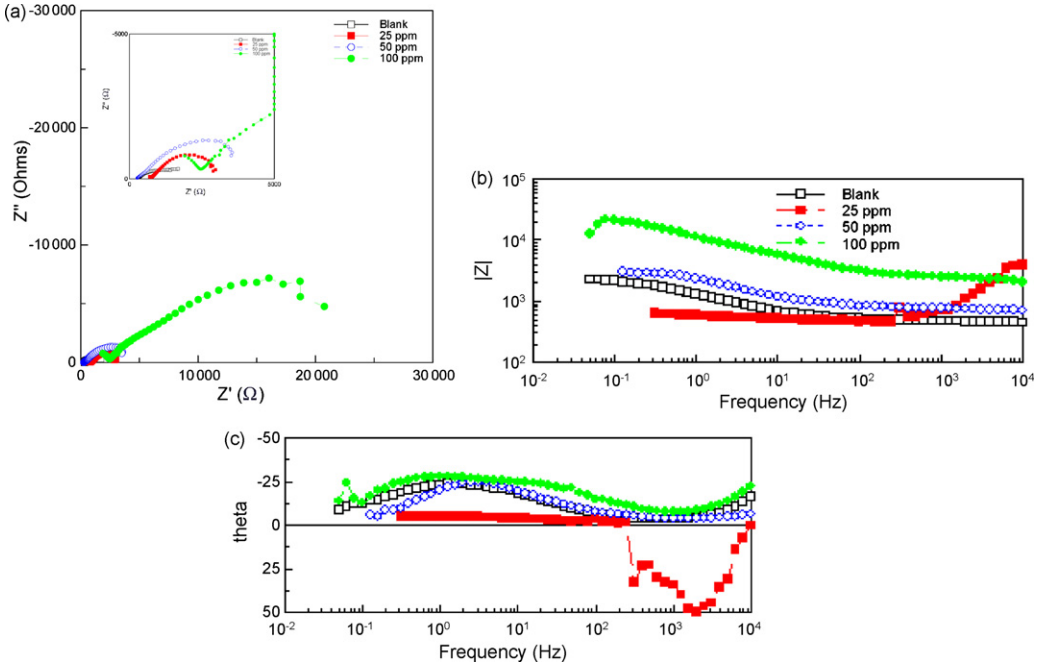

Fig. 7. Impedance diagram (a) Nyquist plots, (b) Bode modulus and (c) Bode phase angle plots diagrams for API 5L-X60 steel in diesel–water mixtures containing different concentrations AAQ derivative (compound **7**).

Table 5
Impedance data for carbon steel API 5L-X60 in diesel–water mixtures in presence of AAQ derivatives (compounds **5–7**)

Compounds	Concentration (ppm)	R_{HF} ($\Omega\,cm^2$)	C_{HF} ($F\,cm^2$)	R_{LF} ($\Omega\,cm^2$)	C_{LF} ($F\,cm^2$)
Compound	25	1,503	1.56×10^{-4}	570	1.15×10^{-8}
5	50	4,299	1.38×10^{-6}	2,706	2.20×10^{-9}
	100	27,185	2.27×10^{-5}	1,851	4.08×10^{-7}
Compound	25	14,344	2.19×10^{-5}	6,949	5.76×10^{-9}
6	50	7,168	1.51×10^{-5}	4,764	4.30×10^{-9}
	100	54,658	3.34×10^{-6}	27,012	6.11×10^{-7}
Compound	25	1,979	4.63×10^{-5}	862	3.74×10^{-9}
7	50	2,894	1.67×10^{-4}	782	3.21×10^{-6}
	100	16,194	1.33×10^{-5}	3,950	5.98×10^{-9}
Blank (no inhibitor)		508	5.72×10^{-7}	934	3.68×10^{-4}

sidered as three layers. First layer is pipeline (electrode), second layer synthesized derivatives and the third layer is diesel–water interface. At anodic areas iron dissolves as Fe^{2+} (Eq. (2)). This reaction is rapid in most media [55]:

$$Fe \rightarrow Fe^{2+} + 2e^- \quad (2)$$

Redox activity natures of synthesized compounds takes the anodically produced two electrons and form the semiquinone and hydroquinone (Scheme 3).

The hydroquinone is highly unstable, it looses two electrons and it returns back to the original state of quinone (cyclic process) that two electrons are taken by bacteria [18] for respiratory process (Scheme 4). The interaction of quinone model compounds or humus substances on the bacterial life cycle was already reported by Cervantes et al. [56–58]. Besides, anodically produced Fe^{2+} ions form the coordinate ligand with hetero atoms (nitrogen and oxygen) present in the synthesized compounds. Subsequently due to the lack of electrons, the cathodic reaction is suppressed. The inhibition effect of these compounds is attributed to the adsorption of the inhibitor molecules on the metal surface. It can be concluded that the corrosion of steel (API 5L-X60) in diesel–water system containing fatty acid substituted aminoanthraquinone inhibits corrosion due to the adsorption of these compounds on the steel surface through their lone pair of electrons and π-electrons of the aromatic ring. All the studied aminoanthroquinone derivatives show the inhibition efficiency of 50–90% in the concentration range of 25, 50 and 100 ppm. It is obvious from table that as the inhibitors concentration increased; resistance of inhibitor layer is increased. However, at 25 ppm concentration, the octanoic acid substituted 1-aminoanthraquinone shows lower efficiency in comparison with other inhibitors due to less surface coverage. The increase in carbon chain increases the corrosion inhibition efficiency. The order of inhibitor efficiency is compound **5** (C_8) < compound **6** (C_{10}) < compound **7** (C_{18}).

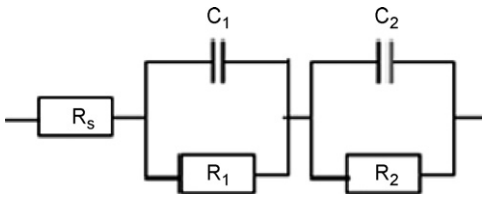

Fig. 8. Corresponding equivalent circuit for API 5LX-60 in diesel–water system.

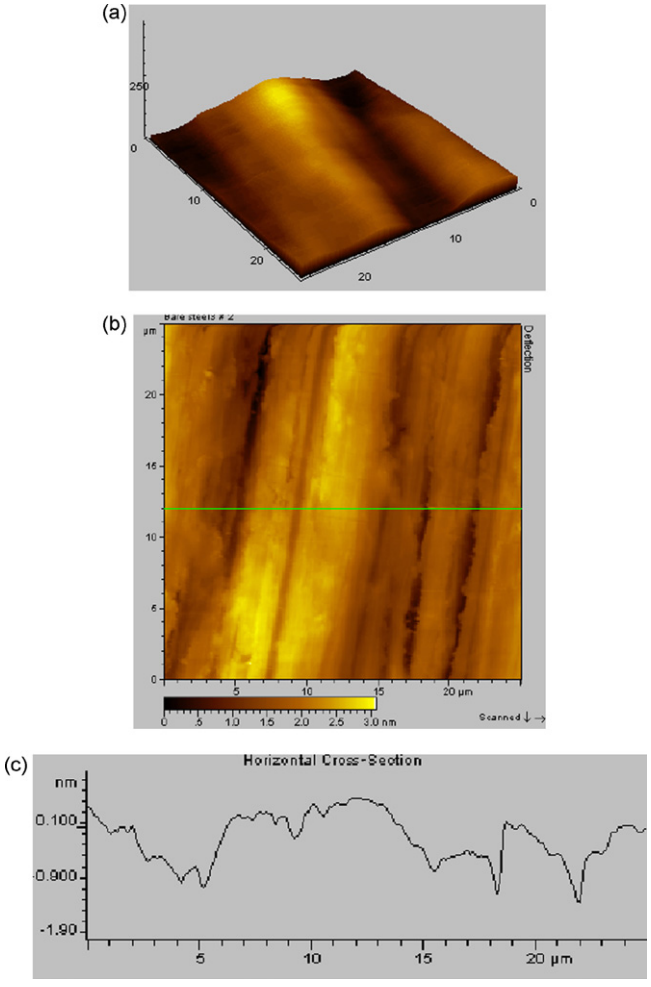

Fig. 9. Cross-sectional profiles of the API 5L-X60 surface in diesel–water mixture: (a) in the absence of 1-aminoanthraquinone (AAQ) derivatives (3D view), (b) surface topography of API 5L-X60 in the absence of AAQ derivative (2D view) and (c) height profile of the API 5L-X60 surface, which is made along the line marked in the corresponding (b).

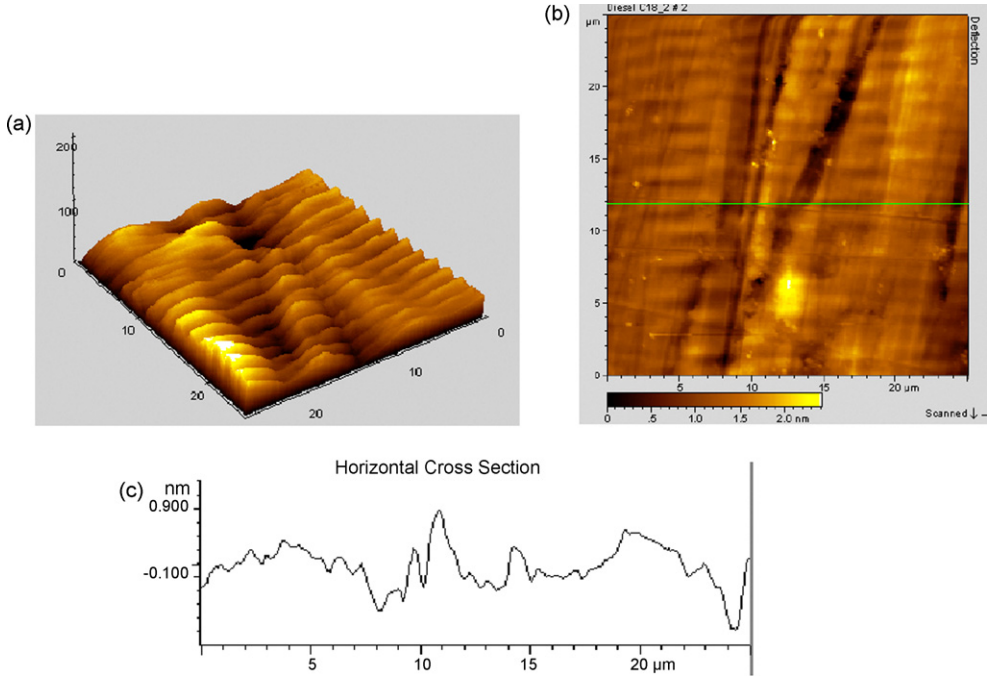

Fig. 10. AFM pictures of the morphology of the electrode (API 5L-X60) obtained after 8 h of immersion in diesel–water mixture of AAQ derivative (compound **7**) at 50 ppm: (a) in the presence of 1-aminoanthraquinone (AAQ) derivative (3D view), (b) surface topography of API 5L-X60 in the presence of AAQ derivative (2D view) and (c) height profile of the API 5L-X60 surface, which is made along the line marked in the corresponding (b).

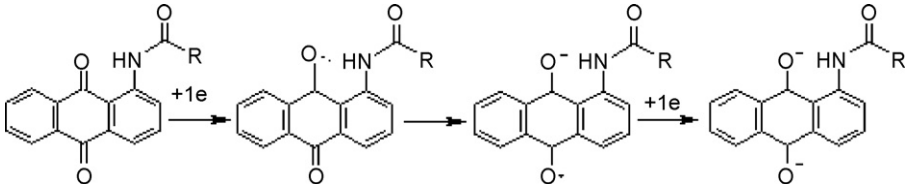

Scheme 3.

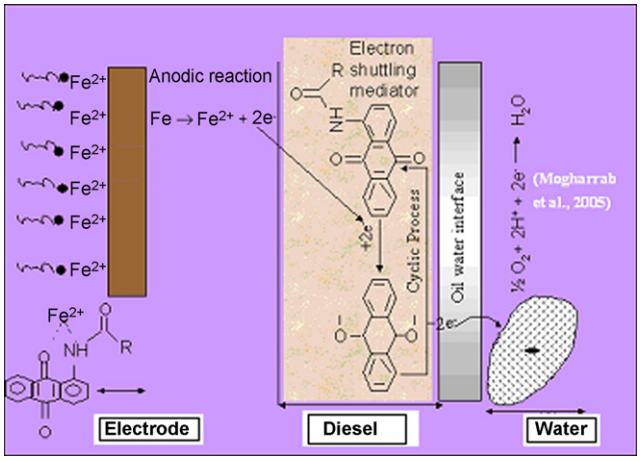

Scheme 4.

4. Conclusions

Oleic acid substituted 1-aminoanthraquinones are found to be good inhibitors for carbon steel (API 5L-X60) corrosion in diesel–water mixtures. Among the three 1-aminoanthraquinone derivatives studied, oleic acid substituted aminoanthraquinone offers higher inhibition efficiency. Polarization and impedance studies also reveal that oleic acid substituted 1-aminoanthraquinone derivative gave better corrosion inhibition than the other synthesized derivatives (compounds **5** and **6**). The synthesized compounds (**5**–**7**) are anodic inhibitors, which bring down the corrosion rate by adsorption mechanism. AFM study also confirms the film formation of the synthesized compounds (compounds **5**–**7**) on the metal surface.

Acknowledgements

The authors wish to express their thanks to the Director, CECRI, Karaikudi 630006, for his kind permission. One of the authors N. Muthukumar thanks CSIR-HRDG for the award of Senior Research Fellowship. The authors are thankful to Dr. S. Sathyanarayanan and Dr. J. Mathiarasu for the help rendered in electrochemical and AFM experiments, respectively. The authors also thank Mr. S.P. Monaharan for the valuable help on fitting of impedance parameters to improve the electrochemical part in the paper.

References

[1] W. Durnie, B. Kinsella, R. De Marco, A. Jefferson, J. Electrochem. Soc. 146 (1999) 1751.
[2] F. Bentiss, M. Lagrenee, M. Traisnel, Corrosion 56 (2000) 733.
[3] V.S. Sastri, Corrosion Inhibitors: Principles and Applications, John Wiley & Sons, New York, 1998.
[4] E.C. French, Mater. Perform. 37 (1978) 20.
[5] I.L. Rosenfeld, Corrosion Inhibitors, McGraw-Hill, New York, 1981.
[6] H.H. Uhlig, R.W. Rivie, Corrosion and Corrosion Control, Wiley, New York, 1985.
[7] P.J. Clewlow, J.A. Haselgrave, N. Carruthers, EP Patent 0,526,251 A1, 1992.
[8] B. Sanyal, Prog. Org. Coat. 9 (1981) 165.
[9] R.W. Revie (Ed.), Uhlig's Corrosion Handbook, 2nd ed., John Wiley & Sons Inc., New York, 2000.
[10] W. Frenier, F.B. Growcock, V.R. Lopp, Corrosion 44 (1988) 590.
[11] F.B. Growcock, W.W. Frenier, Proc. Electrochem. Soc. 86–87 (1986) 104.
[12] A. Cizek, Mater. Perform. 33 (1991) 56.
[13] R.F. Monroe, C.H. Kucera, B.D. Oates, US Patent 3,007,454 (1963).
[14] B.J. Little, P.A. Wagner, F. Mansfeld, Microbiologically Influenced Corrosion, NACE International, Houston, TX, 1997.
[15] D.H. Pope, E.A. Morris III, Mater. Perform. 34 (1995) 23.
[16] N. Muthukumar, S. Mohanan, S. Maruthamuthu, P. Subramanian, N. Palaniswamy, M. Raghavan, Electrochem. Commun. 5 (2003) 421.
[17] A. Navarro, Mol. Aspect. Med. 25 (2004) 37.
[18] R.M. Christie, Colour Chemistry, RSC, Cambridge, UK, 2001.
[19] B. Kampmann, Y. Lian, K.L. Klinkel, P.A. Vecchi, H.L. Quiring, C.C. Soh, A.G. Sykes, J. Org. Chem. 67 (2002) 3878.
[20] P. Terech, R.G. Weiss, Chem. Rev. 97 (1997) 3133.
[21] S. Norvez, F.G. Tournilhac, P. Bassoul, P. Herson, Chem. Mater. 13 (2001) 2552.
[22] V. Prasad, K. Krishnan, V.S.K. Balagurusamy, Liq. Cryst. 27 (2000) 1075.
[23] K.S. Raja, V.A. Raghunathan, S. Ramakrishnan, Macromolecules 31 (1998) 3807.
[24] K. Krishnan, V.S.K. Balagurusamy, Liq. Cryst. 27 (2000) 991.
[25] S. Kumar, J.J. Naidu, Liq. Cryst. 29 (2002) 1369.
[26] S. Kumar, J.J. Naidu, S.K. Varshney, Liq. Cryst. 30 (2003) 319.
[27] M.A. Tius, J. Gomezgaleno, X.Q. Gu, J.H. Zaidi, J. Am. Chem. Soc. 113 (1991) 5775.
[28] N. Mogharrab, H. Ghourchian, Electrochem. Commun. 7 (2005) 466.
[29] T.P. Hoar, R.P. Khera, Proceedings of the European Symposium on Corrosion Inhibitors, vol. Suppl. (3), University of Ferrara, N.S. Sez, 1961, p. 73.
[30] R.D. Desai, R.N. Desai, J. Indian Chem. Soc. 33 (1956) 559.
[31] H.S. Huang, H.F. Chiu, A.L. Lee, C.L. Guo, C.L. Yuan, Bioorg. Med. Chem. 12 (2004) 6163.
[32] Annual Book of ASTM standards, in: Standard practice for preparation, cleaning and evaluating corrosion test specimens (G 1-90), Section 03.02, 2001, p. 15.
[33] S. Papavinasam, R.W. Revie, M. Attard, A. Demoz, H. Sun, J.C. Donini, Mater. Perform. 39 (2000) 58.
[34] D.W. Marquardt, J. Soc. Ind. Appl. Math. 11 (1963) 431.
[35] E. Rodriguez de Schiapparelli, B.R. de Meybaum, Mater. Perform. 19 (1980) 47.
[36] M. Ma, Y. Sun, G. Sun, Dyes Pigments 58 (2003) 27.
[37] T. Philipovaa, C. Ivanovaa, Y. Kamdzhilova, María T. Molinab, Dyes Pigments 53 (2002) 219.
[38] B. Nguyen, P.L. Gutierrez, Chem. Biol. Interact. 74 (1990) 139.
[39] D. Barasch, O. Zipori, I. Ringel, I. Ginsburg, A. Samuni, J. Katzhendler, Eur. J. Med. Chem. 34 (1999) 597.
[40] I.D. Raistrick, Electrochim. Acta 35 (1990) 1579.
[41] H.A. Sorkhabi, S.A. Nabavi-Amri, Electrochim. Acta 47 (2002) 2239.
[42] H.A. Sorkhabi, T.A. Aliyev, S. Nasiri, R. Zareipoor, Electrochim. Acta 52 (2007) 5238.
[43] A. Popova, E. Sokolova, S. Raicheva, M. Christov, Corros. Sci. 45 (2003) 33.
[44] A.P. Yadav, A. Nishikata, T. Tsuru, Corros. Sci. 46 (2004) 169.
[45] Y. Chen, W.P. Jepson, Electrochim. Acta 44 (1999) 4453.
[46] A. Hassanzadeh, A.Z. Isafahani, K. Movassaghi, H.A. Sorkhabi, Acta Chim. Slov. 51 (2004) 305.
[47] T. Hong, Y. Chen, Y.H. Sun, W.P. Jepson, Mater. Corros. 52 (2001) 590.
[48] E.M.-C. Cafferty, N. Hackerman, J. Electrochem. Soc. 119 (1972) 146.
[49] K.F. Khaled, N. Hackerman, Electrochim. Acta 48 (2003) 2715.
[50] A.A. Gewirth, B.K. Niece, Chem. Rev. 97 (1997) 1129.
[51] I.C. Oppenherm, D. Trevor, C.E.D. Chidsey, P.L. Trevor, K. Sieradzki, Science 254 (1991) 688.
[52] J. Li, D. Lampner, Colloids Surf. A 154 (1999) 227.
[53] H.H. Teng, P.M. Dove, C.A. Orme, J.J. De Yoreo, Science 282 (1998) 724.
[54] A. Leng, M. Stratmann, Corros. Sci. 34 (1993) 1657.
[55] J.C. Scully, The Fundamentals of Corrosion, 3rd ed., Pergamon Press, Oxford, UK, 1990.
[56] F.J. Cervantes, Quinones as Electron Acceptors and Redox Mediators for the Anaerobic Biotransformation of Priority Pollutants, Wageningen University, The Netherlands, 2002, ISBN 90-5808-567-8, p. 162.
[57] F.J. Cervantes, S.V. Velde, G. Lettinga, J.A. Field, FEMS Microbiol. Ecol. 34 (2000) 161.
[58] F.J. Cervantes, W. Dijksma, T. Duong-Dac, A. Ivanova, G. Lettinga, J.A. Field, Appl. Environ. Microbiol. 67 (2001) 4471.